# The Yb protein defines a novel organelle and regulates male germline stem cell self-renewal in *Drosophila melanogaster*

Akos Szakmary,[1] Mary Reedy,[1] Hongying Qi,[2,3] and Haifan Lin[1,2,3]

[1]Department of Cell Biology, Duke University Medical School, Durham, NC 27710
[2]Yale Stem Cell Center and [3]Department of Cell Biology, Yale University School of Medicine, New Haven, CT 06520

*Yb* regulates the proliferation of both germline and somatic stem cells in the *Drosophila melanogaster* ovary by activating *piwi* and *hh* expression in niche cells. In this study, we show that Yb protein is localized as discrete cytoplasmic spots exclusively in the somatic cells of the ovary and testis. These spots, which are different from all known cytoplasmic structures in *D. melanogaster*, are evenly electron-dense spheres 1.5 µm in diameter (herein termed the Yb body). The Yb body is frequently associated with mitochondria and a less electron-dense sphere of similar size that appears to be RNA rich. There are one to two Yb bodies/cell, often located close to germline cells. The N-terminal region of Yb is required for *hh* expression in niche cells, whereas the C-terminal region is required for localization to Yb bodies. The entire Yb protein is necessary for *piwi* expression in niche cells. A double mutant of *Yb* and a novel locus show male germline loss, revealing a function for Yb in male germline stem cell maintenance.

## Introduction

Stem cells are characterized by their ability to both self-renew and generate a large number of differentiated progeny. Tissue stem cells usually operate at a steady state, producing one daughter stem cell and one differentiated cell through each division. The division of stem cells is largely controlled by their inductive microenvironment, termed the stem cell niche, which is formed by stable supporting cells often called niche cells (for reviews see Lin, 2002; Morrison and Spradling, 2008). The concept of a stem cell niche was first proposed for the human hematopoietic system (Trentin, 1970). A major challenge in stem cell biology is to define the properties of niche cells and mechanisms through which they regulate the behavior of stem cells.

The organization of niche cells and their essential function in regulating stem cell self-renewal were first defined in the *D. melanogaster* ovary (Lin and Spradling, 1993, 1997; Cox et al., 1998; Xie and Spradling, 1998, 2000; King and Lin, 1999). The *Drosophila* ovary and testis are essentially tubular structures, with the apical end consisting of somatic niche cells that are in contact with germline stem cells (GSCs; Lin, 2004; for review see Lin, 2002). Each *D. melanogaster* ovary consists of 16–18 tubular structures called ovarioles. In each ovariole, 8–10 terminal filament (TF) cells form a stack at the very anterior end (Fig. 1, A–D). Adjacent to them are five to six cap cells that cover the anterior side of two to three GSCs. Oogenesis is initiated when a GSC divides asymmetrically to produce a daughter GSC and a differentiating daughter cell termed the cystoblast. The cystoblast then undergoes four rounds of synchronous divisions with incomplete cytokinesis to produce a germline cyst that contains 16 cells interconnected by cytoplasmic bridges called ring canals (for review see Deng and Lin, 2001). As a 16-cell cyst moves to the middle region of the germarium, two to three somatic stem cells (SSCs) at the periphery of this region divide to produce a monolayer of follicle cells that encapsulate the cyst to form an egg chamber (Margolis and Spradling, 1995). The egg chamber then buds off of the germarium and continues to grow and mature. In the *D. melanogaster* testis, the 10–12 anterior somatic niche cells form a

Correspondence to Haifan Lin: haifan.lin@yale.edu

Dr. Reedy died on 8 August 2008.

Abbreviations used in this paper: GSC, germline stem cell; SMN, survival of motor neuron; snRNP, small nuclear RNP; SSC, somatic stem cell; TF, terminal filament.



The Rockefeller University Press $30.00
J. Cell Biol. Vol. 185 No. 4 613–627
www.jcb.org/cgi/doi/10.1083/jcb.200903034

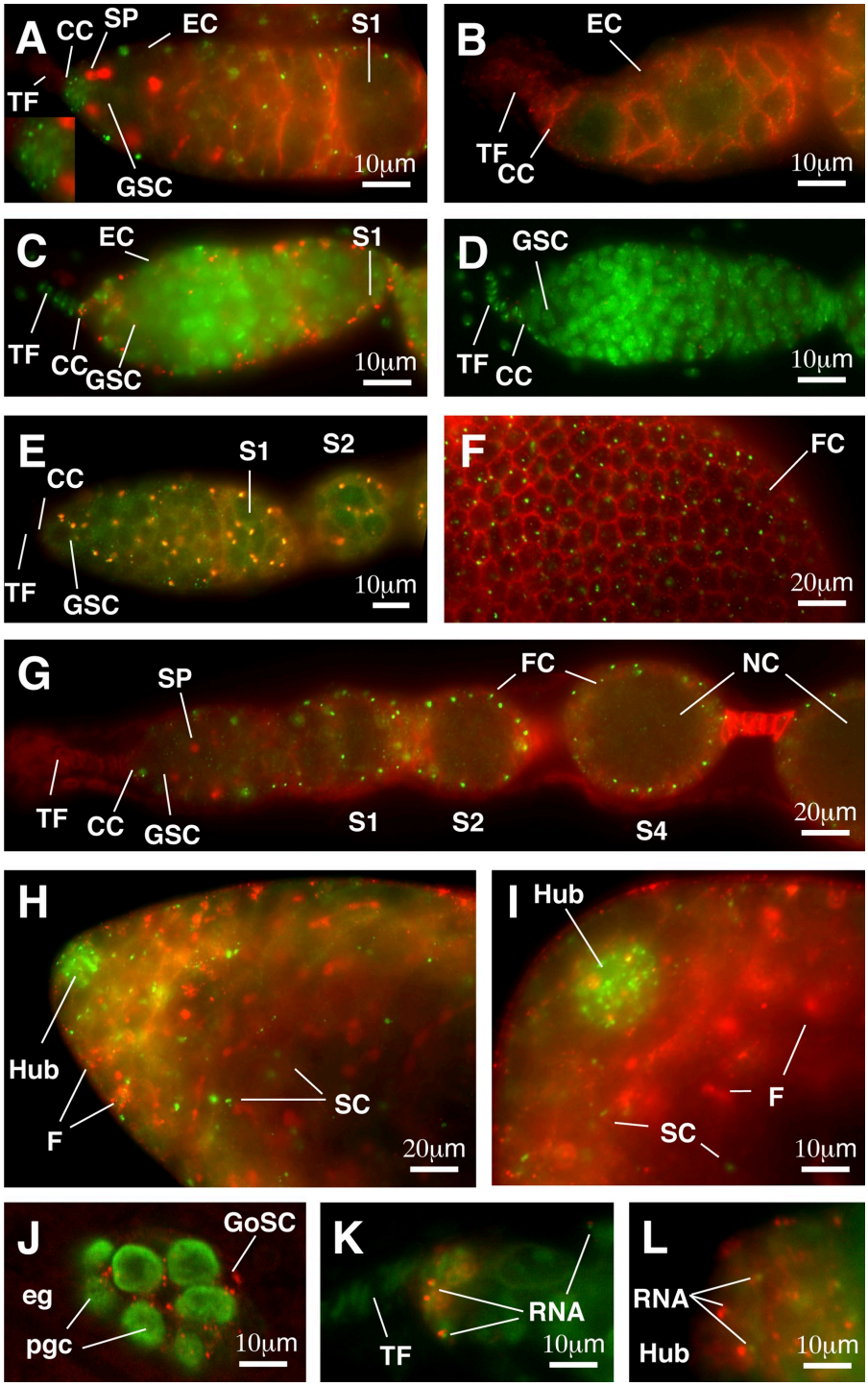


Figure 1. **Yb is localized in discrete spots (Yb bodies) in somatic cells of ovaries and testes.** (A–I) Immunofluorescence images of Yb in wild-type and transgenic ovaries (A and C–G) and wild-type testes (H and I), with a null $Yb^{72}$ mutant ovary (B) shown as a negative control. A and B show a wild-type and a $Yb^{72}$ germarium, respectively, double stained with a Yb (green) antibody to detect Yb and an adducin antibody (red) to visualize spectrosomes (SP) and fusomes (germline-specific organelles) and to outline somatic cells such as escort cells (EC). The inset in A magnifies cap cells (CC) in this panel. C and D show germaria from $w^{1118}$ flies containing or lacking a *FLAG$_5$-Yb* transgene, respectively, double stained for Flag antibody (red) and the DNA dye DAPI (green). E shows a *FLAG$_5$-Yb* transgenic germarium double stained for Flag (red) and Yb (green). F shows part of an egg chamber double stained for Yb (green) and adducing (red), with focus on the follicle cell (FC) surface. G shows a cross-sectioned image of an ovariole double stained for Yb (green) and adducing (red). H shows the apical end of a wild-type testis double stained for Yb (green) and adducing (red). Yb bodies are enriched in the hub cells and are present in somatic cyst cells (SC) but not in germline cells as marked by fusomes (F). I is a higher magnification of H. (J) An area surrounding the gonad in a germ band retraction stage embryo stained with Yb (red) and Vasa (green) is shown. Yb is localized as spheres and spots in gonadal somatic cells (GoSC) but is not detected in primordial germ cells (pgc; green) in the gonad or in extragonadal somatic cells (eg). K and L show RNA-enriched spots (green) associated with the Yb bodies (red) in the germarium and hub region, respectively. S1, S2, and S4 designate stage 1, 2, and 4 egg chambers, respectively. NC, nurse cell.

group called the hub (Fig. 1 H). The hub is surrounded and contacted by six to nine GSCs, each of which is flanked by a pair of SSCs (Jones et al., 2004). A GSC and its two flanking SSCs undergo asymmetrical division in synchrony. After each division, the daughter GSC and SSCs remain in contact with the hub, whereas their sibling cells differentiate into a gonialblast and two somatic cyst cells, respectively. The gonialblast, sandwiched by the two somatic cyst cells, enters four rounds of mitotic divisions to form a 16-cell germline cyst. Subsequent meiotic divisions result in 64 interconnected spermatids.

*D. melanogaster* germ cells contain several specialized cytoplasmic structures, including the spectrosome, fusome, Balbiani body, sponge body, nuage, and U body. The spectrosome (Lin et al., 1994; Lin and Spradling, 1995; Deng and Lin, 1997) is a cytoplasmic organelle rich in membrane skeletal proteins and vesicular materials. In female GSCs, it anchors one pole of the GSC spindle to a niche cell such that the daughter GSC remains associated with the niche cell. The other daughter cell receives a smaller portion of the spectrosome and differentiates to the cystoblast. During the subsequent four cystoblast

divisions, the spectrosome grows into an intercellular structure called the fusome that connects the resulting 16 cells in a germline cyst through ring canals. In addition, the fusome is involved in specifying 1 of the 16 cells in the cyst as an oocyte (Deng and Lin, 1997).

*D. melanogaster* germline cysts also contain Balbiani bodies that are aggregates of mitochondria, ER, Golgi, and other cytoplasmic organelles (Cox and Spradling, 2003). Balbiani bodies have been described for many organisms, with a proposed role in the development of germ plasm. In addition to Balbiani bodies, nurse cells and oocytes contain sponge bodies that are associated with RNA and frequently with mitochondria (Wilsch-Bräuninger et al., 1997). Sponge bodies consist of ER-like cisternae, but they are not specialized Golgi complexes. Instead, they are linked to the assembly and transport of maternal products within the oocyte during *D. melanogaster* oogenesis. At present, it is not known whether Balbiani and sponge bodies are related organelles. Interestingly, the sponge body appears to have overlapping functions with the yeast P body, a cytoplasmic structure which is responsible for programmed mRNA degradation (Sheth and Parker, 2003). This is because Me31B, the *D. melanogaster* orthologue of a key component of the P body in yeast called Dhh1p (an activator of decapping; Coller et al., 2001), is localized to the sponge body (Nakamura et al., 2001). A recently identified U body is also localized in the cytoplasm of the nurse cells and oocyte (Liu and Gall, 2007). U bodies contain major U small nuclear RNPs (snRNPs) and associate with P bodies, suggesting that U bodies may be involved in the assembly and storage of snRNPs and regulation of the snRNP's metabolism.

Another germline-specific organelle is the nuage, a perinuclear structure which is rich in RNA and proteins (Mahowald, 1971). The nuage is made up of electron-dense granules. It contains the putative DEAD box RNA helicase Vasa (Hay et al., 1988; Lasko and Ashburner, 1990) and the RNA-binding protein Aubergine (Harris and Macdonald, 2001) as well as Maelstrom (Findley et al., 2003) and Tudor (Bardsley et al., 1993). Because Vasa and Tudor are also essential components of polar granules, which are germ plasm–specific organelles in the *D. melanogaster* embryo, and because polar granules display nuagelike texture under an electron microscope, the nuage is considered a possible precursor of polar granules and has been suggested to function as an intermediate of cytoplasmic RNP particle assembly (Findley et al., 2003). In contrast to these specialized structures in the germline, no comparable cytoplasmic structure has been described in somatic cells of the ovary or testis.

*Yb* was the first gene identified to regulate two different types of stem cells in an organ (King and Lin, 1999; King et al., 2001). It encodes a novel protein that is specifically required in ovarian somatic niche cells for the self-renewal of both GSCs and SSCs, which produce germline and follicle cells, respectively. Loss of *Yb* function eliminates GSCs and reduces SSC division, whereas overexpression of *Yb* increases GSC number and causes SSC overproliferation. *Yb* appears to achieve this dual regulatory function via the *piwi*- and *hh*-mediated signaling pathways that emanate from the same niche cells to control GSC and SSC division, respectively (King et al., 2001). In addition to its stem cell function, *Yb* is required for follicle cell differentiation by interacting with the *Notch* group of neurogenic genes (Johnson et al. 1995). The *Notch* group genes function in both prefollicular and follicle cells in the germarium as well as in follicle cells in postgermarial egg chambers (Ruohola, et al., 1991). Therefore, *Yb* is also expected to be expressed in all of these somatic cells for its function in follicle cell differentiation. Because *Yb*-null mutant males are fertile, *Yb* is not required in spermatogenesis (King and Lin, 1999). However, it remains to be determined whether Yb is involved in spermatogenesis.

The biochemical mechanism by which Yb achieves its regulation of GSC and SSC divisions is also unknown. *Yb* encodes a novel protein with localized regions bearing similarity to DEAD/DEAH box RNA helicases and a Tudor domain. DEAD/DEAH box RNA helicases are involved in many biological processes (Rocak and Linder, 2004), whereas the Tudor domain is a protein–protein interaction domain (Selenko et al., 2001; Sprangers et al., 2003). To explore the biochemical function of the Yb protein, in this study, we report the determination of its expression and subcellular localization pattern. This has led to the discovery of a novel cytoplasmic structure in the somatic cells of the ovary and testis. Furthermore, we describe discrete functional domains of Yb that are responsible for regulating GSC self-renewal, SSC division, and localization to the Yb body. Finally, we report the novel function of Yb in regulating male GSC self-renewal.

## Results

### Yb protein is localized to discrete spherical structures in ovarian somatic cells

To explore the molecular function of the Yb protein, we examined its expression and localization pattern. Previous RNA in situ hybridization experiments indicated that the *Yb* mRNA is most abundant in TF cells and cap cells of the ovary (King and Lin, 1999). To detect the Yb protein, we produced affinity-purified polyclonal rabbit antibodies against two different Yb peptides (see Materials and methods). Immunofluorescence localization of Yb using these antibodies reveals labeling of discrete spots in all somatic cells in the ovary (Fig. 1, A and E–G). These bright spots are present in high density in the cap cell region and are less dense in the follicle cell layer. However, they are absent from many TF cells. In addition to the spots, a low level of diffuse labeling is detectable in the cytoplasm of both somatic and germline cells.

We verified that the bright, discrete spots but not the diffuse staining represent the Yb protein by the following three additional and independent criteria. First, in the $Yb^{72}$ mutant ovary, in which the Yb protein is truncated upstream of the antibody epitope regions, no discrete Yb spot is detectable, yet the low level of diffuse staining still persists (Fig. 1 B). The much smaller spots seen in Fig. 1 B (which is shown at a three times higher magnification than Fig. 1 A) are spectrin-rich spheres that have been reported for *Yb* mutants (King and Lin, 1999). Second, when an N-terminal $His_6$-Flag–tagged *Yb* transgene that fully rescues the defects of *Yb* mutants (see Materials and

methods and Fig. 5) was stained using three different monoclonal anti-Flag antibodies and a polyclonal Flag antibody, the same staining pattern was observed (Fig. 1 C). The Flag-positive spots are again not detectable in the sibling flies that do not carry the *$His_6$-Flag-Yb* transgene (Fig. 1 D). Third, we constructed a new N-terminal 5× Flag–tagged *Yb* transgene that also fully rescues the *Yb* mutant (see Materials and methods). In this transgene, each Flag is separated by 3 aa residues. When ovaries from flies carrying this transgene were costained by a polyclonal Flag antibody and an anti-Yb antibody, the two antibodies labeled the same discrete spots (Fig. 1 E). Once again, these spots were no longer detectable by anti-Flag antibody in the sibling flies that lack the transgene (unpublished data).

Inspection of the discrete Yb antibody–reactive spots at high magnification revealed that they have a distinctive shape and are present singly or in pairs in each cell. The high density of the spots in the cap cell region (Fig. 1, A, C, E, and G) is the result of the small size and squamous shape of these cells, whereas the one to two spots/cell distribution is clearly seen in the larger follicle cells that envelop individual egg chambers (Fig. 1, F and G). This distribution is clearly seen even in a low magnification image focused on the follicle cells at the surface of an egg chamber (Fig. 1 F). It is also evident in a sagittal section image of an ovariole (Fig.1 G), in which the Yb spots highlight the somatic cells in germaria and egg chambers.

### Yb protein is also localized to discrete spheres in somatic cells of the *D. melanogaster* testes

Although *Yb* mutant males are normal and fertile, previous RNA hybridization and Northern blot analyses indicate that *Yb* is expressed in the testis (King and Lin, 1999). To examine the expression of the Yb protein in the testis, we conducted similar immunofluorescence microscopy to the wild-type *D. melanogaster* testis. Like in the ovary, the Yb protein is localized in discrete spots (Fig. 1, H and I). Moreover, these spots are highly concentrated in hub cells (the cap cell equivalents in the testis) and present in somatic cyst cells (the follicle cell equivalents in the testis), but they are not detectable in the germline. This testicular expression pattern of Yb, which is parallel to its ovarian expression pattern, indicates that the Yb protein might perform the same function in females and males, even though such function may be redundant in males.

### The Yb-containing sphere is specifically present in gonadal somatic cells in embryos

To examine whether the Yb-containing spheres also exist during early gonadogenesis, we examined the Yb expression in embryos by double staining wild-type embryos for Yb and Vasa, a germ cell marker. The Yb protein is clearly localized as conspicuous spheres only in the gonadal somatic cells, but Yb expression is not detected in primordial germ cells or any extragonadal somatic cells (Fig. 1 J). Both the size and morphology of the Yb spheres in the embryonic gonadal somatic cells are very similar to those in the adult ovaries and testes, suggesting that, in the embryo, the Yb-containing sphere is specifically present in the gonadal somatic cells.

### The Yb-containing sphere does not colocalize with known cytoplasmic organelles in *D. melanogaster*

To examine whether the Yb-containing spheres present any known cytoplasmic organelles, we conducted immunocolocalization experiments of Yb and markers of the known cytoplasmic organelles in the *D. melanogaster* reproductive system. Double labeling of 5× Flag–tagged Yb transgenic fly ovaries with anti-Flag antibody and one of the antibodies against markers of the ER (Trap-α; Nicchitta et al., 1991), the nuage (Vasa; Lasko and Ashburner, 1990), the P body (Tral; Wilhelm et al., 2005), the sponge body (Me31B; Nakamura et al., 2001), and the U body (dLsm11; Liu and Gall, 2007) reveals that the Yb-containing spherical structure does not colocalize with any of these structures (Fig. 2). The results, together with electron microscopic analysis (see next section), indicate that the Yb-containing sphere represents a novel cytoplasmic organelle.

### The Yb-containing sphere represents a novel cytoplasmic organelle in gonadal somatic cells

To further investigate the subcellular localization and function of the Yb protein, we conducted immunoelectron microscopy. Ovaries of 5× Flag–tagged Yb transgenic flies were dissected and stained with the anti-Flag antibody and labeled by a secondary antibody conjugated with both 1.4-nm gold particles and a fluorescent label (see Materials and methods). The combination of these two labels allowed visualization of the same sample by both light and electron microscopy. Immunoelectron microscopy revealed that the Yb protein is localized in discrete electron-dense structures in all somatic cells in the germarium (Figs. 3 and 4), including cap cells (Fig. 3, A–E), escort stem cells and escort cells in region I (Figs. 3 A and 4 A), follicle stem cells (also known as SSCs) in region IIa (Figs. 3 A and 4 C), invaginating prefollicular cells in region IIb (Figs. 3 A and 4, E and F), and follicle cells in region III (Figs. 3 A and 4 G). In addition, the Yb-enriched, electron-dense structures are also present in follicle cells of postgermarial egg chambers (unpublished data). We termed these novel structures Yb bodies.

In all of these somatic cell types, Yb bodies show a relatively uniform morphology and localization pattern. Yb bodies are evenly electron-dense round structures, with diameters around 1.5 μm (Figs. 3 and 4). They do not contain membranes, microtubules, microfilaments, or ribosomes, morphological features which are obvious under conventional transmission electron microscopy (Fig. 3, compare B with E; and Fig. 4, compare A with B and C with D). There are one or two Yb bodies per cell, usually in close proximity to mitochondria. In cap cells and SSCs, at least 90% of Yb bodies are adjacent to an unusual round structure of similar size with lower electron density (Figs. 3, B and C; and 4 C). In some cases, the gold labeling of Yb flanks this less electron-dense structure, suggesting that Yb protein may form a toroid encircling other components in cap cells and SSCs. Cap cells often contain one Yb body that is located at the apex region near the TF cells (Fig. 3, B and C) and a second Yb body located adjacent to GSCs (Fig. 3 D). In prefollicular and follicle cells, Yb bodies

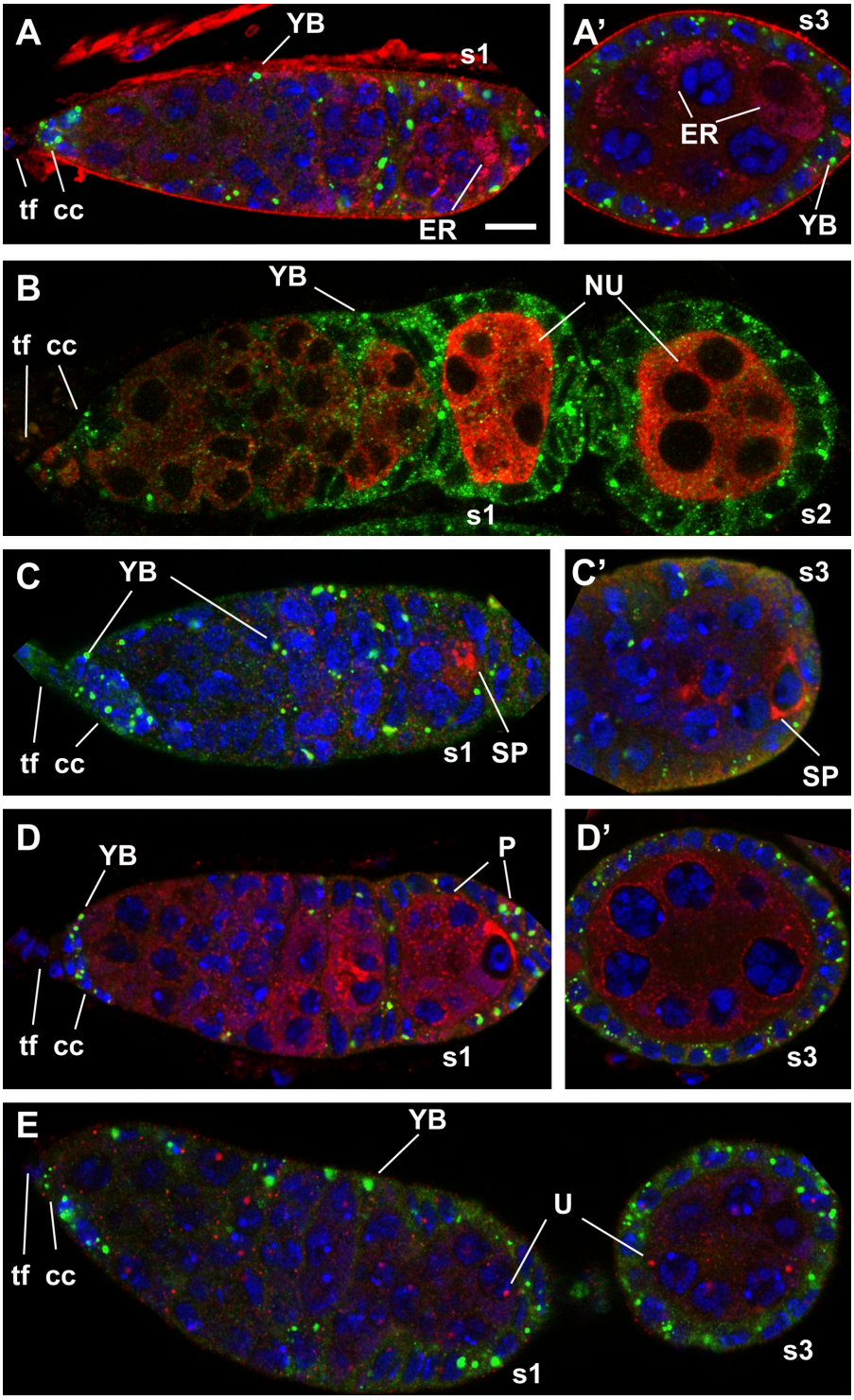


Figure 2. **Yb-containing spheres do not co-localize with known organelles in the *D. melanogaster* ovary.** (A–E) Immunofluorescent costaining of Yb (green) and a marker (red) of the ER (A and A′), the nuage (NU; B), the sponge body (SP; C and C′), the P body (P; D and D′), or the U body (U; E) in wild-type germaria and early stage egg chambers. All of the germaria and egg chambers were oriented with the apical side to the left and the basal side to the right. tf, TF cells; cc, cap cells. s1, s2, and s3 designate stage 1, 2, and 3 egg chambers, respectively. Bar, 10 μm.

are closely associated with mitochondria (Fig. 4, E–G). In addition, the Yb body tends to be located adjacent to germline cells (Figs. 1 G and 4, A and B).

The even electron density of the Yb body resembles that of nuages and sponge bodies, which are two types of germline-specific organelles enriched in proteins and RNAs. However, the shape and the location of the Yb body are very different from nuages and sponge bodies. Because nuages and sponge bodies have been implicated in RNA-related processes, we suspected that Yb bodies may have similar functions. To examine whether the Yb body contains RNA, we costained the whole-mount wild-type ovaries with SYTO RNASelect fluorescent cell stain to visualize RNA and the anti-Yb antibody to identify the Yb body (see Materials and methods). Indeed, Yb bodies in both ovaries and testes are often closely apposed to a spherical structure highly enriched in RNA (Fig. 1, K and L). The size and the association of this RNA-rich structure correspond to the less electron-dense structure that is associated with the Yb body

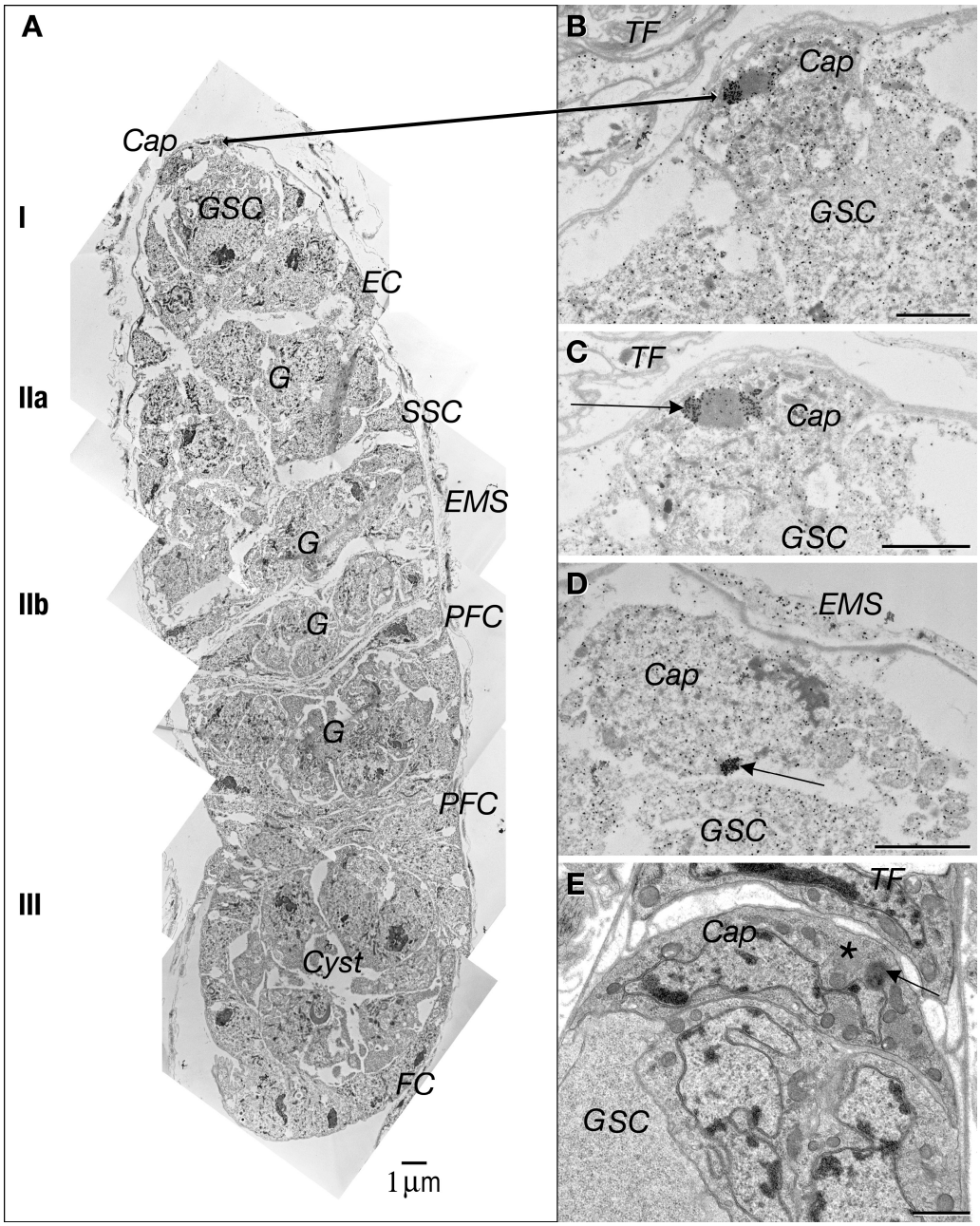


Figure 3. **Electron microscopy of *D. melanogaster* germaria reveals the Yb body as a novel cytoplasmic structure in ovarian somatic cells.** (A) A montage of immunoelectron micrographs of a germarium, with regions I, IIa, IIb, and III marked, after permeabilization and labeling Yb with an AlexFabAu probe. The epithelial muscle sheath (EMS) surrounds the germarium. In region I, the cap cell (Cap) contacts a GSC that is flanked by escort cells (EC). In region IIa, germline cysts (G) occupy the central area, and the SSCs are located on the IIa–IIb border. Region IIb includes three disk-shaped germline cysts surrounded by somatic prefollicle cells (PFC). Region III is a stage 1 egg chamber with a germline cyst containing an oocyte and nurse cells surrounded by follicle cells (FC). The characteristic punctate distribution of fluorescent staining (Fig. 1) is matched by the strong gold labeling of Yb in a specific subcellular structure by immunoelectron microscopy. (B–D) The intense immunogold labeling of the Yb body (arrows) in the Cap cells is shown. Partial serial sections show gold labeling of the Yb body on one side of a less electron-dense sphere (B) or flanking it (C) or as a dense round cluster of gold on the side of the cap cell contacting the GSC (D). (E) Transmission electron micrograph showing the characteristic dense, round Yb body in Cap cells (arrow). The less electron-dense round structure (asterisk) frequently seen beside the denser structure is never labeled by gold. Bars, 2 μm.

in cap cells and SSCs. The close association of the Yb body with the RNA-rich structure suggests that these two structures might be involved in RNA-related processes.

To quantify the Yb protein distribution between the Yb body and the rest of the cytoplasm, we counted the number of gold particles in the Yb body versus the rest of the cytoplasm. In cap cells and other somatic cells, 93.1 ± 1.9% of gold particles are in the Yb body, whereas only 6.9 ± 1.9% of gold particles are in the rest of the cytoplasm. This quantification indicates that almost all Yb protein molecules are localized to the Yb body, which is consistent with the immunofluorescence staining analysis that the diffuse anti-Yb staining does not represent the Yb protein.

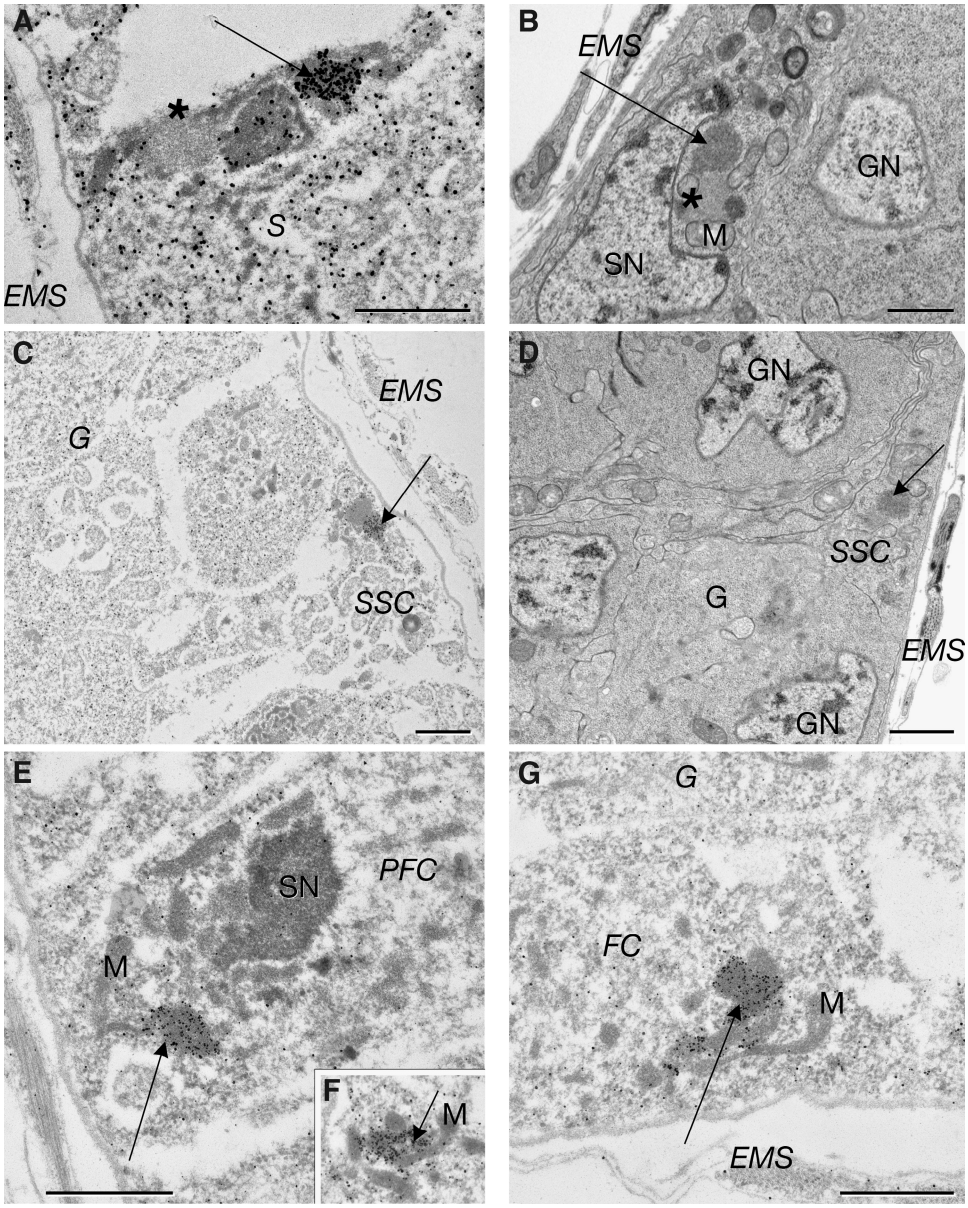


Figure 4. **Electron microscopy of the *D. melanogaster* germarium revealing Yb bodies in regions II and III.** (A) An immunoelectron micrograph of the frequently observed association of a Yb body (arrow) with a less electron-dense round structure (asterisk), a denser round structure, and mitochondria in somatic inner sheath cells (S) in region IIa. (B) A similar structure in an escort cell (arrow) seen by transmission electron microscopy. An adjacent gray spherical body (asterisk) presumably corresponds to the RNA-enriched spot in Fig. 1 J, based on its size, location, and association with the Yb body. (C) SSCs at the region IIa–IIb boarder show gold labeling (arrow) of a Yb body on one side of a less electron-dense structure. (D) A similar structure in an SSC (arrow) seen by transmission electron microscopy. (E and F) Immunoelectron micrographs showing that Yb bodies (arrows) in prefollicular cells are usually associated with mitochondria (M). (G) A Yb body (arrow) in follicle cells (FC) in region III associated with mitochondria. EMS, epithelial muscle sheath; G, germline cyst; GN, germline nucleus; PFC, prefollicle cell; SN, somatic nucleus. Bars, 2 μm.

### Yb is involved in male GSC maintenance

Although Yb protein localizes in a comparable pattern in ovaries and testes (Fig. 1), null *Yb* mutations do not result in sterility in males (Fig. 5, A and B). Thus, if *Yb* performs similar functions in males, another protein or pathway must exist to compensate for *Yb* function in the mutant males. To search for this compensatory gene, we discovered that *Yb* mutant flies became sterile when they were also homozygous for a P-element insertional line called *P[myc-piwi]G38* (herein abbreviated *G38*), in which *P[myc-piwi]* designates the P-element construct containing a functional *myc*-tagged *piwi* transgene, whereas *G38* designates this particular insertional line (Cox et al., 2000). Immunofluorescence microscopic analysis of the $Yb^{72}$*;G38* double mutant further revealed that its testes are often completely, and less often nearly completely, depleted of the germline (Fig. 5). In the case of nearly complete depletion, there are only a small number of arrested early spermatogenic cells. Similar, although somewhat less severe, defects are also seen for the $Yb^{1}$*;G38* double mutant (unpublished data). These defects clearly indicate that functional GSCs are not maintained during spermatogenesis.

The *Yb;G38* synthetic phenotype is likely caused by the disruption of a gene at the insertion site by *P[myc-piwi]* but not caused

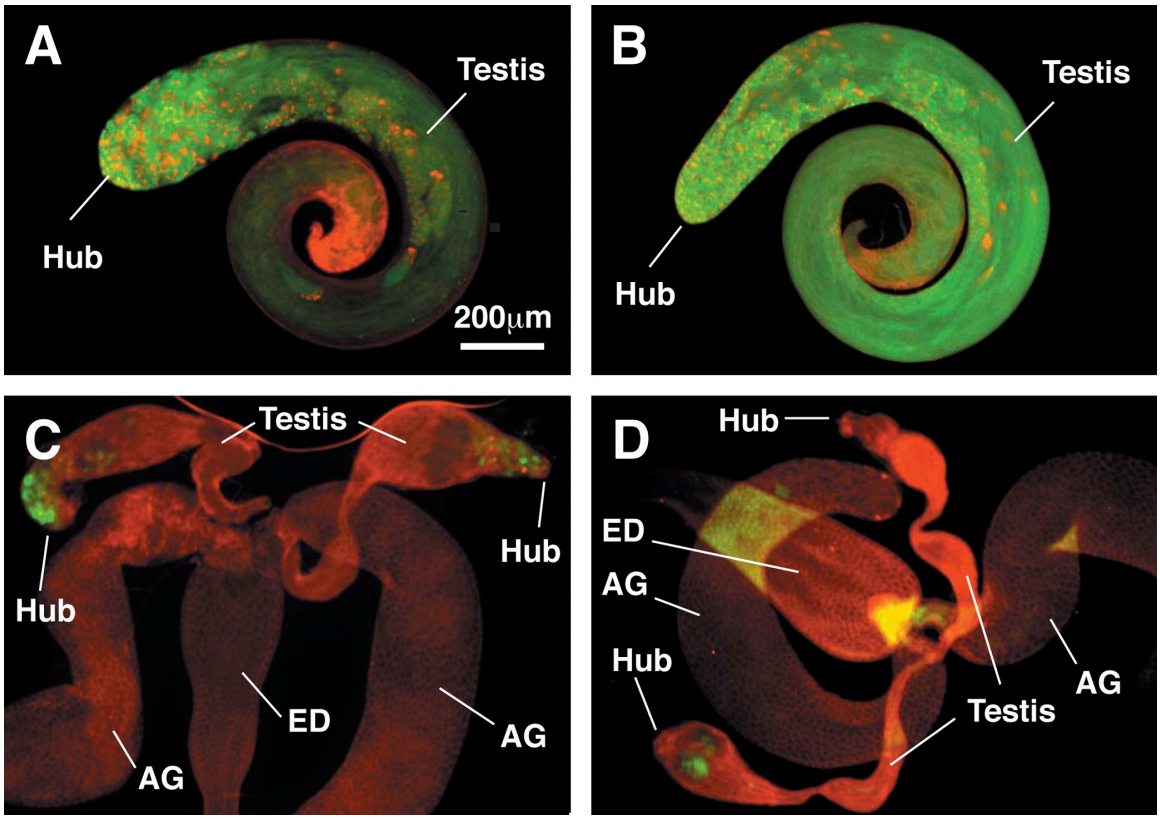


Figure 5. **Yb regulates GSC self-renewal in the testis.** All samples were stained for the germline marker Vasa (green) and the cytoskeletal marker 1B1 (red) and are shown under the same magnification. (A and B) The testes of the homozygous $Yb^{72}$ mutant (A) or homozygous for both *P[myc-piwi]G38* and *P[myc-piwi]G47* insertions (B) are morphologically normal, and these males are fully fertile. (C and D) However, homozygous $Yb^{72}$;*P[myc-piwi]G38* testes lose their germline shortly after eclosion and are almost completely sterile. Examples of a weaker (C) and a more severe (D) $Yb^{72}$;*P[myc-piwi]G38* phenotype are shown. C and D also contain the accessory glands (AG), which are similar to wild-type testes in size, as a comparison for reduced size the degenerating testes. ED, ejaculatory duct.

by the expression of the *myc-piwi* transgene or any other effect of the inserted *P* construct. This is based on the following two lines of evidence. First, the same construct inserted at other genomic sites such as *P[myc-piwi]G47* also expresses the functional *myc-piwi* at normal levels (Cox et al., 2000). However, mutants homozygous for *P[myc-piwi]* at these sites and *Yb* do not display the synthetic male sterile phenotype. This indicates that the synthetic effect is insertion site specific but not caused by the expression of *myc-piwi* or another effect of the construct. Second, wild-type flies homozygous for both *G38* and *P[myc-piwi]G47* insertions are normal and fertile (Fig. 4 B). Because both *G38* and *P[myc-piwi]G47* express functional *myc-piwi*, this indicates that even six copies of functional *piwi* genes (four transgenic and two endogenous) in flies do not affect male fertility (Cox et al., 2000; Megosh et al., 2006). Thus, the loss of fertility in these flies is caused by the disruption of a gene by the P element at the insertion site rather than by the increased dosage of *piwi*. Together, these observations reveal that Yb is involved in GSC maintenance, even though this role is not essential.

### The N-terminal region of Yb is required for *hh* expression, whereas the entire Yb protein is needed for *piwi* expression and SSC maintenance

The Yb protein contains a 166-aa region (residues 396–562) homologous to the DEAD/DEAH box RNA helicases and a 127-aa Tudor-like domain (residues 817–944; Fig. 5). The DEAD/DEAH box RNA helicases family has many members and is involved in numerous processes. However, the only known *D. melanogaster* proteins that contain both DEAD/DEAH box RNA helicase and Tudor domains are Homeless (also known as Spindle-E) and two uncharacterized proteins with similarities to Yb (CG31755 and CG11133).

To explore the functions of the different regions of the Yb protein, we generated cDNA genomic DNA transgenes that express various deleted or point-mutated variants of Yb and used them for in vivo rescue experiments. The deletion/point mutation series were designed according to Yb sequence features. Fig. 6 shows a schematic summary of all of these constructs sequentially aligned from the N to C terminus. For comparison, the mutational sites of the four known *Yb* mutant alleles are also indicated on the wild-type transgene. None of these transgenes was able to rescue the fertility of the null $Yb^{72}$ allele beyond slight improvement (Fig. 6), indicating that all regions of Yb are essential for fertility.

Despite this, we noticed that the phenotypes of the ovaries varied depending on whether they carried either an N-terminal deletion or other mutations. This suggested different effects of mutations on oogenesis. Specifically, N-terminal deletions show fused egg chambers, suggesting underproliferation of follicle cells that resembles the *hh* mutant phenotype (Fig. 7;

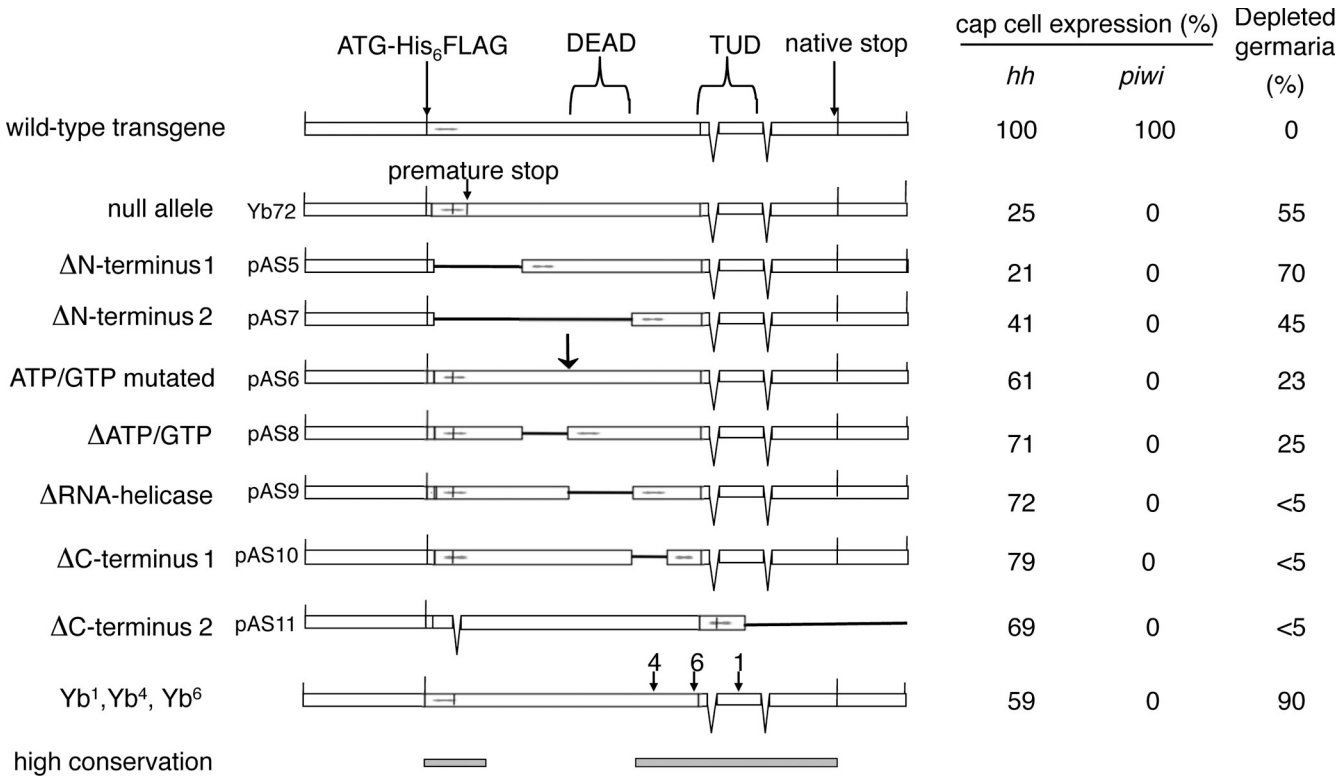


Figure 6. **Summary of Yb deletional analysis.** All mutant *Yb* alleles and transgenes are drawn to scale. Open boxes represent exon genomic/cDNA sequences. Intronic sequences were represented by spaces between exons and delineated by the V-shaped thin lines that connect exons and indicate a splicing pattern. The ability of each construct to rescue *hh* and *piwi* expression and the germarial defect is correspondingly listed on the right side of the construct, with the percentage indicating the percentage of germaria with cap cells expressing *hh* or *piwi*. The positions of the $Yb^1$, $Yb^4$, and $Yb^6$ mutations are also labeled on the wild-type cDNA genomic Yb fusion transgene. The two gray bars in the bottom indicate the N-terminal 150-residue and C-terminal 470-residue regions of the Yb protein that are highly conserved among *Drosophila* species. The arrow indicates the position of the point mutation in the P-loop ATP/GTP-binding sequence. TUD, Tudor-like domain.

Forbes et al., 1996). Because Yb-controlled *hh* expression is mostly responsible for follicle stem cell division (King et al., 2001), this raises the possibility that the N-terminal region of Yb is more responsible for regulating *hh* expression. However, transgenes with more C-terminal deletions show pinched and split egg chambers, often with very few nuclei, suggesting that follicle proliferation is improved, but germline cells are underproliferated (Fig. 8). Therefore, we tested these transgenes for their ability to restore *hh* expression in cap cells or *piwi* expression in somatic niche cells. N-terminal deletions often showed no rescue of *hh* expression in cap cells (Figs. 6 and 7, C–E). All other transgenes tested restored *hh* expression in cap cells (Fig. 8, B and C). However, none of the deletion transgenes rescued *piwi* expression in somatic niche cells (Figs. 6 and 8, D and E). Therefore, the N-terminal region is required for *hh* expression and follicle cell proliferation, whereas the entire Yb protein is necessary for *piwi* expression and GSC self-renewal during oogenesis.

To further identify functionally important regions of Yb, we compared its sequences among several *Drosophila* species. We identified Yb homologues in *Drosophila simulans*, *Drosophila yakuba*, *Drosophila erecta*, *Drosophila ananassae*, *Drosophila virilis*, and *Drosophila mojavensis*. (*Drosophila pseudoobscura* genome data [release 1.0] did not contain a homologue because of a sequencing gap.) The Yb sequences of more closely related species, *D. simulans* and *D. yakuba* (2.6 myrs and 10 myrs separation from *D. melanogaster*), revealed a very strong conservation for the first N-terminal 150 aa, followed by a lower degree of conservation in short stretches of fewer than 10 aa residues, up to the RNA helicase domain (Fig. 6). The Yb proteins show very high homology in the last 470 residues at the C-terminal region. This pattern of homology corresponds well with our deletion/mutation analysis, suggesting that the N-terminal 150 aa residues may be important for *hh* expression in cap cells, whereas the C-terminal 470 residues may be essential for Yb protein localization via binding to protein partners.

### $Yb^1$, $Yb^4$, and $Yb^6$ mutant proteins fail to localize to the Yb body

The $Yb^1$, $Yb^4$, and $Yb^6$ alleles are epithelial muscle sheath–induced point mutations that are genetic null (Young and Judd, 1978; Mohler and Carroll, 1984; King and Lin, 1999). Sequence analysis shows that $Yb^1$ is a missense mutation in Arg972 that is conserved in all Tudor domains so far studied and therefore is likely to be essential for Tudor domain function. The crystal structure of the Tudor domain in the survival of motor neuron (SMN) protein indicates that this domain likely functions as a protein–protein-binding domain (Selenko et al., 2001, Sprangers et al., 2003). $Yb^4$ and $Yb^6$ are missense mutations at residues 747 and 858, respectively, located between the DEAH box RNA helicase domain and the Tudor domain. Using the polyclonal antibody against native Yb protein, we

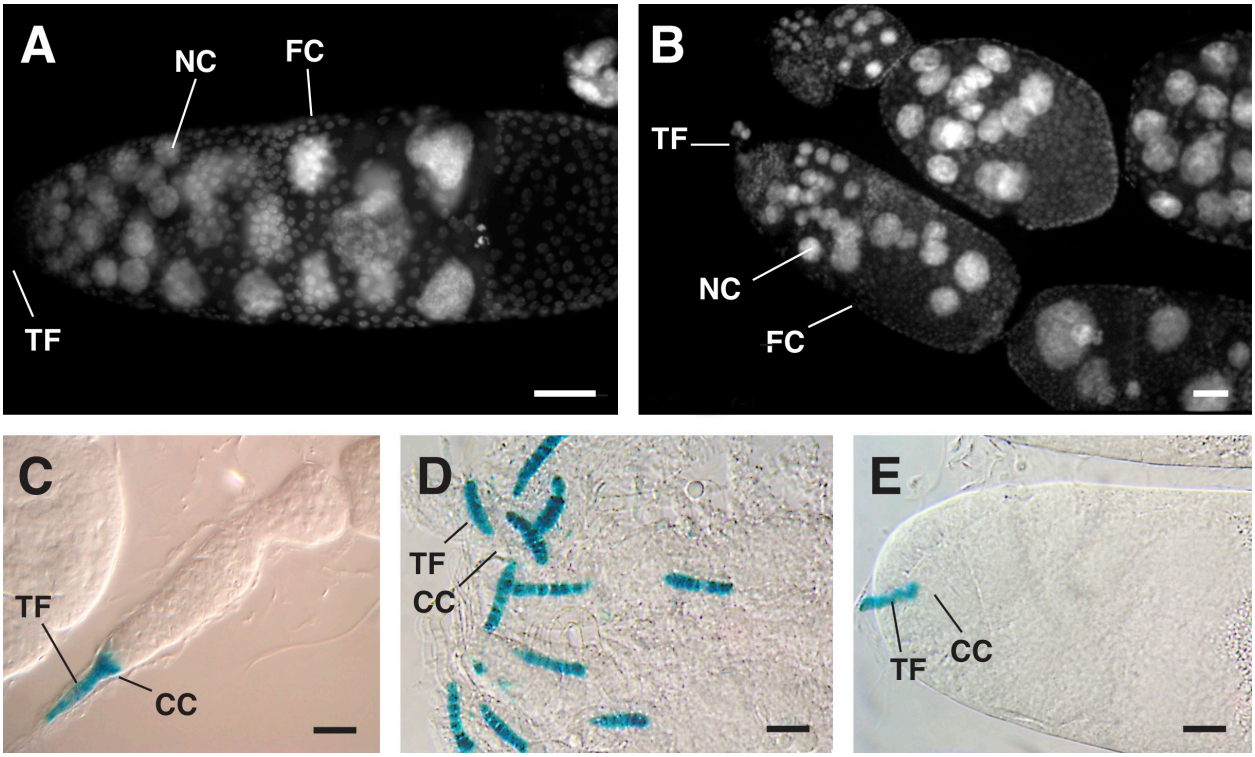


Figure 7. **The N-terminal region of Yb is required for HH expression in cap cells.** (A and B) DAPI images of $Yb^{72}/Yb^{72}$ ovarioles carrying a transgene with an N-terminal deletion (pAS5 in A and pAS7 in B). Underproliferation of follicle cells (FC) is evident by the presence of fused egg chambers, each of which contains multiple germline cysts. The germline development is not obviously affected, as indicated by the presence of groups of 16-nurse cell (NC)/oocyte clusters, with the ploidy of each group increasing in a gradient fashion from apical to basal region of the ovariole. (C–E) The expression of the *hh-lacZ* reporter gene in ovarioles that are wild-type (C) or $Yb^{72}/Yb^{72}$ carrying the pAS5 (D) or pAS7 (E) transgene is shown. In the wild-type ovariole, both cap cells (CC) and TF cells show robust *hh* expression. However, in the mutant ovarioles, *hh* expression is conspicuously missing from cap cells, even though its expression in TF cells is normal. This TF-only expression of *hh* is similar to that of $Yb^{72}/Yb^{72}$ ovarioles (King et al., 2001), indicating that the N-terminal–deleted *Yb* transgenes do not restore the expression of *hh* in cap cells. Bars, 20 µm.

first examined whether these mutant proteins are stably expressed. Western blot analysis indicates that $Yb^1$, $Yb^4$, and $Yb^6$ proteins are expressed as expected full-length proteins (unpublished data).

We then examined whether the amino acid changes affect the ability of the protein to localize to the Yb body. As shown in Fig. 9, $Yb^1$, $Yb^4$, and $Yb^6$ mutations eliminate the localization of Yb protein to the Yb body in both females and males. This finding suggests that these mutations disrupt the ability of Yb protein to localize or organize the Yb body and that the localization of Yb protein in the Yb body may be essential for its function. Interestingly, the deletion transgene pAS7 that expresses a $His_6$-Flag–tagged Yb lacking its N-terminal half upstream of the $Yb^4$ mutation site still showed localization to Yb bodies (Fig. 9 F). Therefore, the sequences required for proper integration into the Yb body are located in the C-terminal half of the protein, possibly in the 470 highly conserved region, with resides mutated by $Yb^1$, $Yb^4$, and $Yb^6$ mutations crucial for the localization of Yb to the Yb body or the organization of the structure. This Yb body association region is distinct from the aforementioned sequences shown to be essential for *hh* expression in cap cells.

## Discussion

In this paper, we have reported a novel and distinctive subcellular structure that localizes the Yb protein and defined Yb functional regions responsible for *hh*- and *piwi*-mediated niche signaling and for subcellular localization as well as revealed its role in the self-renewal of male GSCs. These results expand our understanding of cellular and molecular mechanisms involved in niche signaling, which regulates GSC division in *D. melanogaster*, with implications for niche signaling in other stem cell systems.

### Yb body as a novel organelle

Subcellular localization experiments revealed that Yb localizes to a new discrete electron-dense structure in somatic cells of the ovary, testis, and embryonic gonad that we call the Yb body. Immunofluorescence and immunoelectron microscopy reveals that the Yb body is distinct from known cytoplasmic organelles such as endosomes, lysosomes, mitochondria, the ER, nuages, sponge bodies, U bodies, and vesicular elements of the Golgi complex. Moreover, unlike nuages, sponge bodies, and U bodies, Yb bodies are only in the ovarian somatic cells, especially dense in the cap cells, which is consistent with the in situ Yb mRNA localization pattern, but not in the germline. However, the Yb bodies are not abundant in TF cells, in which Yb mRNA is also strongly detectable. This could reflect a differential regulation of Yb mRNA translation in TF and cap cells.

The Yb body shares certain morphological and structural similarities with nuages, sponge bodies, and P bodies (also known as GW bodies in mammalian cells; Eystathioy et al., 2002), all of

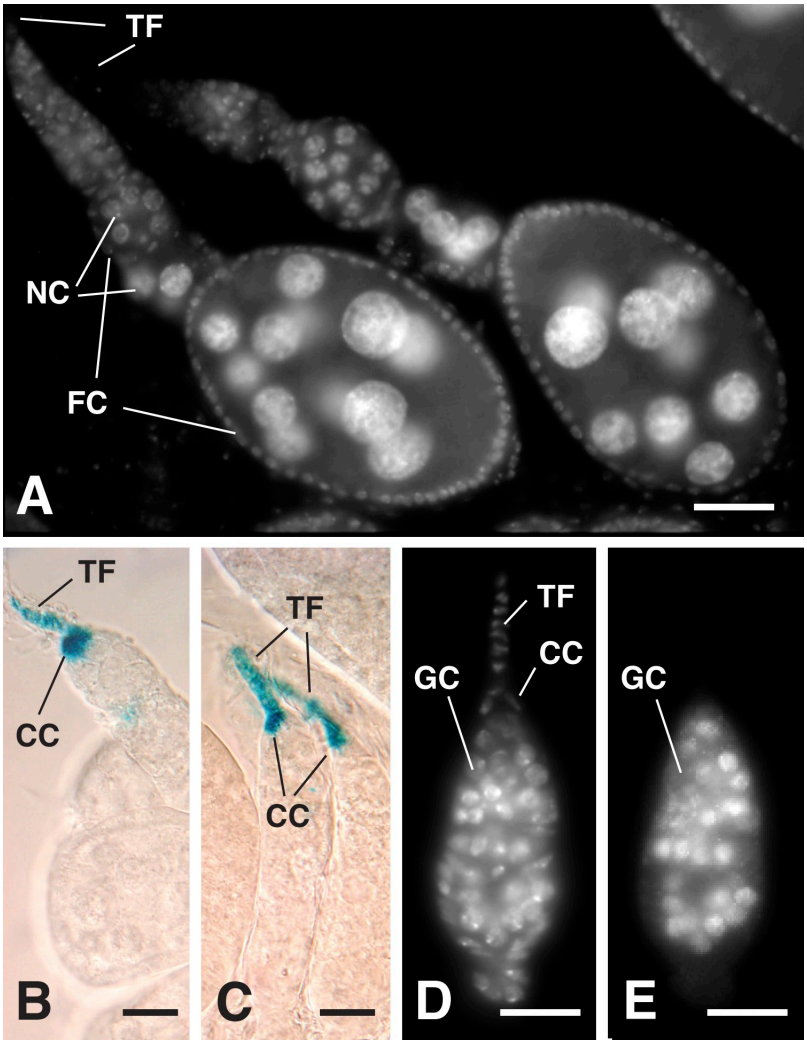


Figure 8. **C-terminal region of Yb is required for PIWI but not HH expression in niche cells.** (A) DAPI image of $Yb^{72}/Yb^{72}$ ovarioles carrying a transgene with a C-terminal deletion (pAS10). These ovarioles show improved follicle cell (FC) proliferation, implicating improved *hh* signaling, which is essential for follicle stem cell division (Forbes et al., 1996). (B and C) Consistent with this, the cap cell (CC) expression of *hh* is fully restored in $Yb^{72}/Yb^{72}$ mutants by introducing a C-terminally deleted Yb (pAS9 in B and pAS10 in C). This suggests that the C-terminal region of Yb is not required for HH expression. (D and E) A $Yb^{72}/Yb^{72}$ germarium, carrying a pAS10 transgene and an *myc-piwi* gene, stained for DAPI (D) and myc-PIWI (E), respectively, is shown. The expression of *piwi* in TF and cap cells is not restored. This is also the case when any other mutant transgene in Fig. 6 is introduced into the $Yb^{72}/Yb^{72}$ mutants (see Fig. 6 for summary). Thus, the full-length Yb protein is required for *piwi* expression. GC, germline cell; NC, nurse cell. Bars, 20 μm.

which are involved in RNA stability and translational control. Nuage is a germline-specific, RNP particle–rich, electron-dense, and cloudlike perinuclear structure that possesses similar electron density and texture to the Yb body. Nuage is a possible polar granule precursor and might function as an intermediate of cytoplasmic RNP particle assembly (Findley et al., 2003). Nuage contains putative Dex/hD box RNA helicases such as Vasa that share partial structural similarities to Yb. It also contains putative RNA-binding proteins such as Aubergine and Tudor. Therefore, the Yb body might be involved in RNA processing.

The sponge body, another germline-specific structure involved in cytoplasmic RNA transport (Wilsch-Bräuninger et al., 1997; Nakamura et al., 2001), is similar to the Yb body in that both are associated with RNA and mitochondria. Unlike the evenly electron-dense texture and spherical shape of the Yb body, the sponge body contains ER-like membrane cisternae. However, Me31B, the *D. melanogaster* orthologue of Dhh1p and a component of the P body in yeast (Coller et al., 2001; Sheth and Parker, 2003), also localizes to the sponge body (Nakamura et al., 2001). The P body is involved in programmed mRNA degradation (Eystathioy et al. 2002; Sheth and Parker, 2003) as well as microRNA and RNAi pathways (Liu et al., 2005; Sen and Blau, 2005; Rehwinkel et al., 2005). The P bodies in yeast and mammalian cells (Eystathioy et al., 2002; Sheth and Parker, 2003) are granular, electron-dense bodies devoid of membranous structures, which are similar to the ultrastructural features of the Yb body. Immunoelectron microscopy further revealed that P bodies contain electron-dense fibrils (Yang et al., 2004). The ultrastructural similarities between nuage, the sponge body, the P body, and the Yb body all hint that the Yb body is involved in RNA-related processes.

The possibility that the Yb body functions in RNA-related process is intriguing. Compartmentalization of mRNA and trans-acting proteins in controlling translation and stability of mRNAs is likely to be important in the *D. melanogaster* ovarian somatic cells (cap cells, prefollicle cells, and postgermarial follicle cells), which must maintain a specific polarity in their contact and communication with neighboring germ cells. Indeed, the Yb body is frequently located near the germline-contacting side of the cytoplasm. It is possible that the Yb body represents a somatic counterpart to the germline-specific organelles such as nuage, sponge bodies, or Balbiani bodies. The Yb body may be involved in regulating the expression of the signaling machinery at the mRNA level. It will be interesting to identify additional protein and, possibly, RNA components of the Yb bodies and to determine

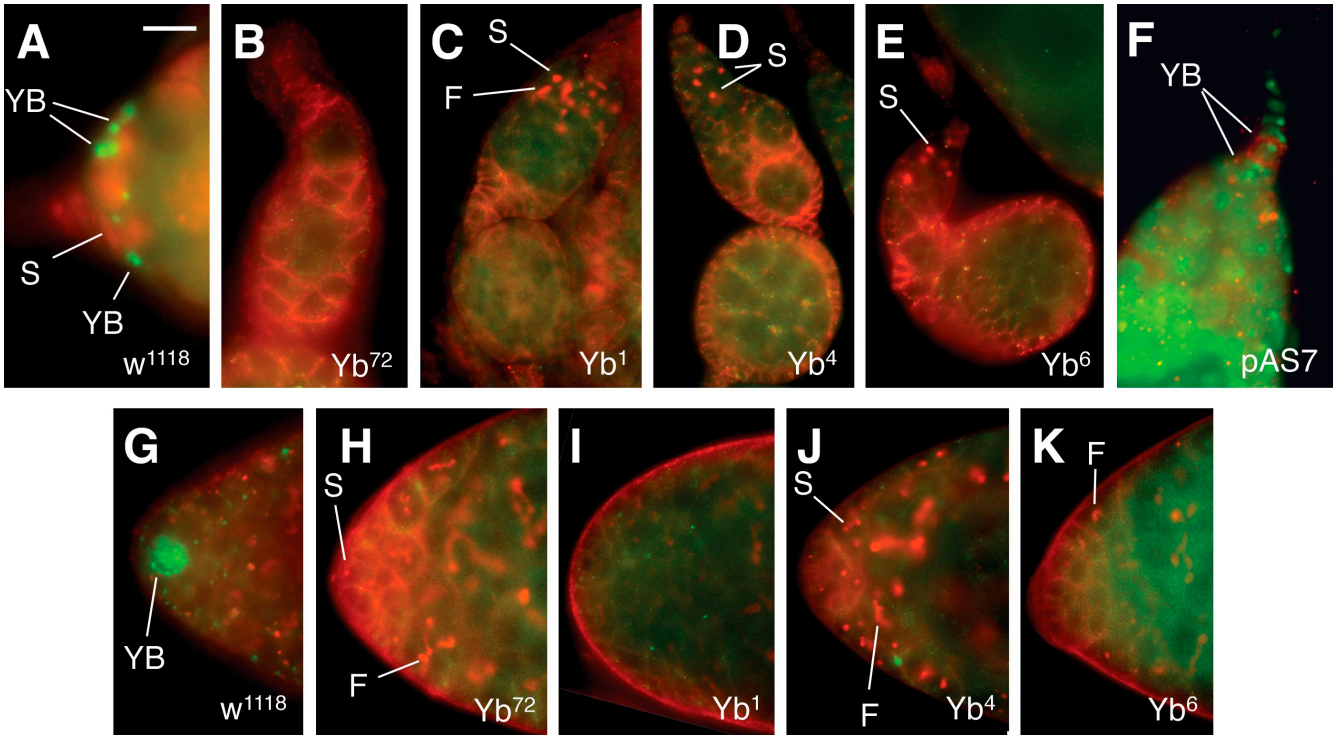


Figure 9. **C-terminal region is required for Yb localization.** This figure shows the localization of mutant Yb proteins encoded by five *Yb* mutant alleles, among which *Yb*$^{72}$ is a premature mutation introducing a stop codon at amino acid residue 134 (King et al., 2001) and *Yb*$^{1}$, *Yb*$^{4}$, and *Yb*$^{6}$ are missense mutations that are genetically null (King and Lin, 1999), whereas the pAS7 transgene encodes the C-terminal half of the Yb protein (Fig. 5). (A–E) Wild-type (A) and *Yb* mutant (B–E) germaria stained for Yb protein (green) and for 1B1 (red) to outline the somatic cells and to label the spectrosome. Yb$^{1}$, Yb$^{4}$, and Yb$^{6}$ mutant proteins are not localized to the Yb body. (F) The localization of the pAS7 mutant Yb protein with the N-terminal half deleted, as detected by anti-His antibody (red) to recognize the Yb body in the wild-type germarium, is shown. The DAPI staining (green) labels the nuclei in the germarium. (G–K) Wild-type (G) and the *Yb* mutant (H–K) testicular apex stained for Yb protein (green) and for 1B1 (red) to outline the somatic cells and to label the spectrosome. Yb$^{1}$, Yb$^{4}$, and Yb$^{6}$ mutant proteins are not localized to the Yb body in the testis, either. F, fusome; S, spectrosome; YB, Yb body. Bar: (A–F) 10 µm; (G–K) 20 µm.

whether the composition of the Yb body varies in different types of cells and tissues.

### The role of Yb in regulating male GSC self-renewal

The failure of the male GSC maintenance in the *Yb;G38* double mutant but not their corresponding single mutants indicates that Yb and a second gene affected by the *G38* mutation positively regulate the self-renewal of these GSCs in a compensatory manner. This finding provides an opportunity to explore Yb-mediated niche signaling mechanism in regulating male GSC self-renewal by cloning and systematically characterizing the gene disrupted by the *G38* mutation.

### Functional domains of the Yb protein

Sequence homology searches revealed two conserved protein domains in Yb, a putative DEAD/DEAH box RNA helicase domain and a Tudor domain. These two domains are essential for Yb function because the pAS6 mutation in the Walker B motif of the helicase domain and the *Yb*$^{1}$ mutation that mutates an extremely well conserved Arg residue in the Tudor domain to a Gln residue both result in loss of GSC maintenance and failure of the protein localization to the Yb body. The precise function of these domains cannot be predicted from sequence alone. DEAH box RNA helicases domains are found in many proteins and are involved in numerous processes. It has been proposed recently that most of these helicases release proteins from RNA rather than unwinding RNA (Fairman et al., 2004). However, the helicase homologous domain of the Yb protein contains no obvious DEAD box motif (King and Lin, 1999); thus, Yb is unlikely to be an RNA helicase but might still be involved in other RNA-related function. The Tudor domain is currently of unknown function but is present in several RNA-binding proteins (Ponting, 1997). However, based on the structure of the Tudor domain in the SMN protein, it is more likely to mediate protein–protein interaction (Selenko et al., 2001). The Tudor domain of the SMN protein binds to methylated RG tails of SMN proteins with particularly high affinity (Sprangers et al., 2003). Finally, it is rare to see proteins with a combination of a DEAD/DEAH box RNA helicase domain and a Tudor domain. In *D. melanogaster*, two novel and uncharacterized genes, CG31755 and CG11133, encode proteins with this domain combination and share moderate sequence similarity with Yb over most of their lengths. Our search has also revealed CG11133-like genes in *Pan troglodytes* and *Homo sapiens* but no Yb homologue outside of the *Drosophila* genus. In *D. melanogaster*, although the Homeless protein displays little sequence homology to the Yb protein, they share the same domain combination. A short part of the Tudor domain is conserved between Yb and Homeless, but the conserved sequence does include the Arg residue critical

for function. Thus, even though Homeless is known to be involved in RNA localization and possibly translational regulation in the oocyte, considerable effort is needed to elucidate the biochemical activities of Yb.

Although sequence homology analysis has not revealed obvious biochemical activities for Yb, our deletional analysis has defined distinct regions of Yb that are responsible for its three different molecular functions: (1) activation of HH expression in somatic niche cells, (2) activation of PIWI expression in somatic niche cells, and (3) Yb body localization and/or organization. This analysis suggests that Yb is a functionally tripartite protein with the N-terminal half required for *hh* expression in cap cells, the C-terminal half required for Yb localization to Yb bodies, and the entire protein needed for *piwi* expression in somatic niche cells. The Yb body localization function requires the Tudor domain but not the helicase homology domain, yet the PIWI expression function requires both domains, including a conserved ATP/GTP-binding site in the helicase domain. Future studies, including the identification of protein interactors specific to different domains of Yb, should help decipher the biochemical functions of these domains as well as reveal other components of the Yb body.

## Materials and methods

### *Drosophila* strains and culture

All strains were grown at 25°C on yeast-containing molasses/agar medium. The following fly strains were used. The *P[myc-piwi]G38* insertion on the second chromosome, with an expression pattern representative of most *P[myc-piwi]* transgenic lines, was used to visualize PIWI protein localization (Cox et al., 2000). $w^{1118}$ served as the wild-type strain in all experiments unless indicated otherwise. $Yb^{1}$, $Yb^{4}$, and $Yb^{6}$ are previously described *Yb* point mutations (King and Lin, 1999), whereas $Yb^{72}$ is a truncation allele that causes a premature termination of the 1,042-aa Yb protein at residue 134 (King et al., 2001); all of these alleles are considered to be null (King and Lin, 1999; King et al., 2001). The *hh-lacZ* chromosome used is from the Bloomington BL-5530 *ry[506] P{ry[+t7.2]=PZ}hh[P30]* strain. LacZ staining was performed as previously described (Lin et al., 1994).

### Construction of transgenic flies

To produce a $His_6$-Flag epitope fused to the Yb sequence, the following primer pair was purchased from Integrated DNA Technologies: the 5′ $His_6$-Flag primer (5′-TTGCTAGCCGTACATATATTAGGCGCAGCATGCACCATCACCATCACCATGAC-3′) and the 3′ Yb Flag primer (5′-TCTCCAATTGGCTCCTTGTCGTCGTCGTCCTTATAGTC-3′). These primers were phosphorylated, mixed, and filled in by PCR reaction. PCR product of the correct length was gel purified, digested with NheI–MfeI, and inserted into the pJ35 ΔXhoI plasmid. pJ35 ΔXhoI contains only the N-terminal sequence of *Yb* and allows the use of the first MfeI restriction site right after the ATG codon. The resulting $His_6$-Flag–tagged 5′ *Yb* fragment was digested with NheI–BsiWI and used to replace the corresponding sequence in pCa4Stu (genomic Yb rescue fragment), resulting in a P-element transformation vector containing a genomic *Yb* rescue fragment with a $His_6$-Flag sequence after the ATG start codon. This construct completely rescued the phenotype of the $Yb^{72}$ mutant (Fig. 5).

For deletion analysis, the $His_6$-Flag–tagged 5′ *Yb* fragment digested with NheI–BsiWI was also introduced into a NheI–BsiWI-digested pJ35 plasmid (untagged *Yb* cDNA containing Bluescript vector) to yield pJ38 (5′ $His_6$-Flag–tagged *Yb* cDNA containing Bluescript vector). pJ38 was then digested with appropriate restriction enzymes to generate the desired deletion mutants as indicated in Fig. 6. Specifically, vector fragments were blunt-ended by either fill-in or chew-off reactions to retain the appropriate reading frames and then relegated and sequenced. The point mutagenesis in the P-loop ATP/GTP-binding sequence was achieved by PCR with four PCR primers containing the desired mutation, according to the standard protocol of PCR-based targeted mutagenesis. All of the newly constructed *Yb* deletion/mutation sites were introduced into pCa4Stu (genomic Yb rescue fragment) using the unique NheI and Bsu36I sites except for pAS11, which used Bsu36I and a site in Bluescript. All of the resulting transformation plasmids were resequenced over the relevant regions before injection into embryos.

To enhance the sensitivity and specificity for immunodetection of Yb, a DNA sequence of a 5× Flag tag with each Flag epitope separated by 3 aa residues was constructed. To construct this sequence, the following five Flag primer pairs were purchased from Integrated DNA Technologies, annealed in pairs, phosphorylated, and ligated: 1 upper, 5′-GACTATAAGGACGACGACGACAAGACCACCGGA-3′; 1 lower, 5′-CTTGTCGTCGTCGTCCTTATAGTCCATGCTGCG-3′; 2 upper, 5′-GACTATAAGGACGACGACGACAAGACCGGAGGA-3′; 2 lower, 5′-CTTGTCGTCGTCGTCCTTATAGTCTCCGGTGGT-3′; 3 upper, 5′-GACTATAAGGACGACGACGACAAGGGAGCCGGA-3′; 3 lower, 5′-CTTGTCGTCGTCGTCCTTATAGTCTCCTCCGGT-3′; 4 upper, 5′-GACTATAAGGACGACGACGACAAGACCATTA-3′; 4 lower, 5′-CTTGTCGTCGTCGTCCTTATAGTCTCCGGCTCC-3′; 5 upper, 5′-GACTATAAGGACGACGACGACAAGGAGCCAATTGGAGA-3′; and 5 lower, 5′-CTTGTCGTCGTCGTCCTTATAGTCAATAATGGT-3′.

The ligation product of desired length (5× Flag) was gel purified and reamplified with the following Flag primer pairs: 5′ *Yb* ATG Flag primer (5′-TTGCTAGCCGTACATATATTAGGCGCAGCATGGACTATAAGGAC-3′) and 3′ *Yb* flag primer (5′-TCTCCAATTGGCTCCTTGTCGTCGTCGTCCTTATAGTC-3′). The resulting PCR fragment was digested with NheI and MfeI and cloned into the plasmid pJ35 ΔXhoI. As in the $His_6$-Flag–tagged construct, an NheI–BsiW fragment from this plasmid containing the Yb transcriptional regulatory region and the 5× Flag–tagged 5′ part of the Yb open reading frame was used to replace the corresponding sequence in pCa4Stu (genomic Yb rescue construct; King and Lin, 1999), resulting in a P-element transformation vector containing a genomic Yb rescue fragment with a 5× Flag sequence after the ATG start codon. This construct also completely rescued the phenotype of the $Yb^{72}$ mutant.

Transgenes in P-element transformation vectors were introduced into $w^{1118}$ flies via germline transformation (Rubin and Spradling, 1982). The transgenes were injected at the Duke University Model System Genomics Facility (http://www.biology.duke.edu/model-system).

### Staining for RNA in whole-mount ovaries

Ovaries were dissected and fixed for 10 min or 2 h in prechilled methanol at −20°C (no difference was observed between these two fixing times) followed by several washes in 1× PBS. Labeling was performed with SYTO RNASelect green fluorescent cell stain (Invitrogen). All of the following procedures were performed in the dark. Ovaries were incubated for 20 min at RT in a 500-nM solution of the dye in 1× PBS followed by several washes in PBS. Counterstaining with Yb antibody was subsequently performed as described in the next section (beginning with the blocking step).

### Antibody production and affinity purification

MAP-8–conjugated peptides of (H-IKENTPPTSSEDYKAEA) 8× MAP (Yb pep3) and (H-IDTTSLDSIRTVKDSPA) 8-MAP (Yb pep4) were purchased from Invitrogen. These peptides correspond to amino acid residues 187–203 and 322–338 of Yb, respectively. The peptides were each injected into one rabbit by Cocalico Biologicals, Inc. according to standard protocol.

Serum was obtained from rabbits immunized with peptides Yb pep3 (serum DU159) and Yb pep4 (serum DU160). IgG was isolated from both sera by purification on a protein A–Sepharose column (GE Healthcare). Both IgG fractions were further purified through affinity matrix and prepared by cross-linking peptides Yb pep3 and Yb pep4 to Reacti-Gel 6X (Thermo Fisher Scientific). For the cross-linking, 23 mg of peptide Yb pep3 and 10 mg of peptide Yb pep4 were separately incubated with 1 ml of activated resin in 0.1 M sodium carbonate buffer, pH 10, for 24 h at 4°C. The reaction was stopped by incubation with 1 M ethanolamine, pH 10.0, for 24 h. After extensive washing, peptide columns were loaded with the protein A–purified IgG and incubated overnight at 4°C. The columns were washed extensively and then eluted with 0.05 M of Gly buffer, pH 2.5, containing 0.15 M NaCl. Fractions were immediately neutralized with 0.1 vol of 1 M Tris-HCl, pH 8.0, pooled, and dialyzed against a buffer containing 0.025 M Hepes-KOH, pH 7.5, and 0.15 M KCl. The purified antibodies were aliquoted, quick-frozen in liquid nitrogen, and stored at −80°C.

### Immunohistochemistry

Ovaries and testes were dissected, fixed, and stained as previously described (Lin et al., 1994). For immunofluorescence staining, the following antisera were used: polyclonal rabbit anti-Vasa (1:2,000; Hay et al., 1990), monoclonal mouse anti-1B1 (which recognizes spectrosomes and fusomes; 1:1; Zaccai and Lipshitz, 1996), polyclonal rabbit anti–α-spectrin (1:200; Byers et al., 1987), monoclonal mouse anti-MYC epitope 1-9E10.2 (1:50; Evan et al., 1985), monoclonal mouse anti–Flag M2 (1:300; Sigma-Aldrich), polyclonal rabbit anti–Flag F7425 (1:500; Sigma-Aldrich), monoclonal

mouse anti-Me31B (1:400; provided by A. Nakamura, RIKEN Center of Developmental Biology, Kobe, Japan; Nakamura et al., 2001), polyclonal rabbit anti-Tral (1:750; provided by J. Wilhelm, University of California, San Diego, La Jolla, CA; Wilhelm et al., 2005), polyclonal rabbit dLsm11 (1:3,000; provided by J.G. Gall, Carnegie Institute of Washington, Baltimore, MD; Liu and Gall, 2007), and polyclonal rabbit Trap-α (1:200; provided by C. Nicchitta, Duke University, Durham, NC; Nicchitta et al., 1991). Affinity-purified rabbit anti–Yb pep3 antibody was used at 1:250 dilution. All of the fluorescence-conjugated secondary antibodies were purchased from Jackson ImmunoResearch Laboratories and used at 1:200 dilution except for Alexa Fluor 488 (Invitrogen), which was used at 1:500 dilution. Immunofluorescently labeled samples were also counterstained with DAPI as described previously (Lin and Spradling, 1993). Photomicrographs were taken using either a microscope (Axioplan; Carl Zeiss, Inc.) with the image captured by a cooled charge-coupled device camera (Star-1; Photometrics) or a confocal microscope (LSM510; Carl Zeiss, Inc.) using its built-in camera. Both microscopes use a 10× NA 0.3 Plan-Neofluar, a 20× NA 0.8 Plan-Apochromat, and a 40× NA 1.3 Plan-Neofluar oil differential interference contrast objective for low, medium, and high magnification imaging, respectively. All images were processed using Photoshop (Adobe).

**Transmission electron microscopy**

The conventional transmission microscopy of wild-type germaria was conducted according to Lin et al. (1994) or Reedy and Beall (1993). Images were taken using an electronic microscope (EM420; Philips) in the Department of Cell Biology at Duke University.

**Immunoelectron microscopy**

Ovaries were dissected from 5× Flag–Yb transgenic flies, fixed, and stained with mouse monoclonal anti–Flag M2 antibodies for immunocytochemistry as previously described (Lin et al., 1994). Anti–mouse Nanogold and Alexa Fluor 488 double-conjugated secondary antibodies were used for secondary labeling (1:3). Ovaries were washed, lightly cross-linked with 0.1% glutaraldehyde, and aldehyde quenched with 50 mM Gly in PBS, according to the protocol from Nanoprobes, Inc. Several ovaries were directly inspected by immunofluorescence (Fig. 5 A). The Nanogold labeling of anti–Flag-Yb in the remaining ovaries was enhanced using GoldEnhance from Nanoprobes, Inc. according to the manufacturer's protocols. Subsequently, ovaries were rinsed and fixed with 2% glutaraldehyde in MOPS-buffered mammalian ringer solution for 1 h at RT and rinsed in same buffer and then in 0.1 $MPO_4$ and 10 mM $MgCl_2$, pH 6.1, at 4°C. Secondary fixation was performed in 1% $OsO_4$ in the same $PO_4$ buffer for 1 h on ice. After a water rinse, 2% aqueous uranyl acetate was used as a block stain for 30 min on ice. After a water rinse, tissue was dehydrated in a graded 50–100% ethanol series and infiltrated in Araldite 506 epoxy resin (Tousimis Research Corporation). Germaria and attached early egg chambers were separated from the ovary by microdissection, oriented in puddles of Araldite on sheets of polyethylene, and allowed to partially polymerize to maintain the orientation. Araldite-filled BEEM capsules (BEEM, Inc.) were inverted over the germaria. Several intact ovaries were also embedded. Curing was performed for 48 h at 65°C. 0.5-µm sections were used to guide orientation, and 50-nm thin sections were cut with a diamond knife (Diatome) and mounted on thin carbon films on copper grids. Sections were stained with aqueous 2% $KmnO_4$, rinsed with Pal's bleach and water, and stained with Sato lead (Reedy and Reedy, 1985). Montages of the entire germaria were assembled from low magnification (3,300×) electron micrographs, and the clusters of gold labeling in individual cells were recorded at 10,000–12,000×.

**Western blot analysis**

Flies were dissected and homogenized in 1× sample buffer as previously described (Cox et al., 2000). Samples were boiled for 10 min, centrifuged, and loaded on 10% SDS-PAGE gels. Western blotting was performed according to standard protocol (Sambrook et al., 1989). Antibodies against YB and the Flag epitope were used at a dilution of 1:500 and 1:5,000, respectively.

**BLAST (Basic Local Alignment Search Tool) analysis of sequence homologies**

*Yb* homologues in *D. simulans* and *D. yakuba* were determined by using the GSC BLAST search service website of Washington University, St. Louis (http://genome.wustl.edu), and tBlastN. The genome of *D. pseudoobscura* was screened using the genome browser of the University of California, Santa Cruz (http://genome.ucsc.edu/cgi-bin/hgGateway?db=dp2), but the *D. pseudoobscura* sequence has an apparent gap that uncovers the expected *Yb* homologue. Sequence assemblies for the genomes of *D. erecta*, *D. ananassae*, *D. virilis*, and *D. mojavensis* were BLAST searched using tBlastN developed by C. Jones (University of North Carolina at Chapel Hill, Chapel Hill, NC).

This paper is dedicated to the memory of Dr. Mary Reedy, a wonderful collaborator and friend.

We thank Drs. Brigid Hogan, Vann Bennett, Chris Nicchitta, and Seth Findley for their valuable suggestions on the manuscript, Dr. Jochen Genschel for help with Yb antibody purification, Dr. Zhong Wang for help in BLAST searching sequence assemblies, and Dr. Heather Megosh for help in Western blot analysis of the Yb mutant proteins. We also thank Drs. A. Nakamura, J. Wilhelm, J.G. Gall, and C. Nicchitta for providing Me31B, Tral, dLsm11, and Trap-α antibodies, respectively.

This work is supported by grants from the National Institutes of Health to H. Lin (HD33760) and M. Reedy (R37-AR14317) and from the G. Harold and Leila Y. Mathers Foundation to H. Lin.

Submitted: 6 March 2009
Accepted: 13 April 2009

## References

Bardsley, A., K. McDonald, and R.E. Boswell. 1993. Distribution of tudor protein in the *Drosophila* embryo suggests separation of functions based on site of localization. *Development*. 119:207–219.

Byers, T.J., R.R. Dubreuil, D. Branton, D.P. Kiehart, and L.S.B. Goldstein. 1987. *Drosophila* Spectrin. II. Conserved features of the alpha-subunit are revealed by analysis of cDNA clones and fusion proteins. *J. Cell Biol.* 105:2103–2110.

Coller, J.M., M. Tucker, U. Sheth, M.A. Valencia-Sanchez, and R. Parker. 2001. The DEAD box helicase, Dhh1p, functions in mRNA decapping and interacts with both the decapping and deadenylase complexes. *RNA*. 7:1717–1727.

Cox, R.T., and A.C. Spradling. 2003. A Balbiani body and the fusome mediate mitochondrial inheritance during *Drosophila* oogenesis. *Development*. 130:1579–1590.

Cox, D.N., A. Chao, J. Baker, L. Chang, D. Qiao, and H. Lin. 1998. A novel class of evolutionarily conserved genes defined by piwi are essential for stem cell self-renewal. *Genes Dev.* 12:3715–3727.

Cox, D.N., A. Chao, and H. Lin. 2000. *piwi* encodes a nucleoplasmic factor whose activity modulates the number and division rate of germline stem cells. *Development*. 127:503–514.

Deng, W., and H. Lin. 1997. Spectrosomes and fusomes anchor mitotic spindles during asymmetric germ cell divisions and facilitate the formation of a polarized microtubule array for oocyte specification in *Drosophila*. *Dev. Biol.* 189:79–94.

Deng, W., and H. Lin. 2001. Asymmetric germ cell division and oocyte determination during *Drosophila* oogenesis. *Int. Rev. Cytol.* 203:93–138.

Evan, G.I., G.K. Lewis, G. Ramsay, and J.M. Bishop. 1985. Isolation of monoclonal antibodies specific for human *c-myc* proto-oncogene product. *Mol. Cell. Biol.* 5:3610–3616.

Eystathioy, T., E.K. Chan, S.A. Tenenbaum, J.D. Keene, K. Griffith, and M.J. Fritzler. 2002. A phosphorylated cytoplasmic autoantigen, GW182, associates with a unique population of human mRNAs within novel cytoplasmic speckles. *Mol. Biol. Cell*. 13:1338–1351.

Fairman, M.E., P.A. Maroney, W. Wang, H.A. Bowers, P. Gollnick, T.W. Nilsen, and E. Jankowsky. 2004. Protein displacement by DexH/D "RNA Helicases" without duplex unwinding. *Science*. 304:730–734.

Findley, S.D., M. Tamanaha, N.J. Clegg, and H. Ruohola-Baker. 2003. Maelstrom, a *Drosophila* spindle-class gene, encodes a protein that colocalizes with Vasa and RDE1/AGO1 homolog, Aubergine, in nuage. *Development*. 130:859–871.

Forbes, A.J., H. Lin, P.W. Ingham, and A.C. Spradling. 1996. *hedgehog* is required for the proliferation and specification of somatic cells during egg chamber assembly in *Drosophila* oogenesis. *Development*. 122:1125–1135.

Harris, A.N., and P.M. Macdonald. 2001. *Aubergine* encodes a *Drosophila* polar granule component required for pole cell formation and related to eIF2C. *Development*. 128:2823–2832.

Hay, B., L. Ackerman, S. Barbel, L.Y. Jan, and Y.N. Jan. 1988. Identification of a component of *Drosophila* polar granules. *Development*. 103:625–640.

Hay, B., L.Y. Jan, and Y.N. Jan. 1990. Localization of *vasa*, a component of *Drosophila* polar granules, in maternal-effect mutants that alter embryonic anteroposterior polarity. *Development*. 109:425–433.

Johnson, E., S. Wayne, and R. Nagoshi. 1995. *fs(1)Yb* is required for ovary follicle cell differentiation in *Drosophila melanogaster* and has genetic interactions with the Notch group of neurogenic genes. *Genetics*. 140:207–217.

Jones, D.L., Y.M. Yamashita, C. Schulz, and M.T. Fuller. 2004. Regulation of stem cell self-renewal versus differentiation by a support cell niche: lessons from the *Drosophila* male germ line. *In* Handbook of Stem Cells, vol. 1. R. Lanza, editor. Elsevier Academic Press, Boston. 171–178.

King, F.J., and H. Lin. 1999. Somatic signaling mediated by *fs(1)Yb* is essential for germline stem cell maintenance during *Drosophila* oogenesis. *Development*. 126:1833–1844.

King, F.J., A. Szakmary, D.N. Cox, and H. Lin. 2001. Yb modulates the divisions of both germline and somatic stem cells through *piwi*- and *hh*-mediated mechanisms in the *Drosophila* ovary. *Mol. Cell*. 7:497–508.

Lasko, P.F., and M. Ashburner. 1990. Posterior localization of vasa protein correlates with, but is not sufficient for, pole cell development. *Genes Dev.* 4:905–921.

Lin, H. 2002. The stem-cell niche theory: lessons from flies. *Nat. Rev. Genet.* 3:931–940.

Lin, H. 2004. *Drosophila* female germ line stem cells. *In* Handbook of Stem Cells, vol. 1. R. Lanza, editor. Elsevier Academic Press, Boston. 157–169.

Lin, H., and A.C. Spradling. 1993. Germline stem cell division and egg chamber development in transplanted *Drosophila* germaria. *Dev. Biol.* 159:140–152.

Lin, H., and A.C. Spradling. 1995. Fusome asymmetry and oocyte determination in *Drosophila*. *Dev. Genet.* 16:6–12.

Lin, H., and A.C. Spradling. 1997. A novel group of pumilio mutations affects the asymmetric division of germline stem cells in the *Drosophila* ovary. *Development*. 124:2463–2476.

Lin, H., L. Yue, and A.C. Spradling. 1994. The *Drosophila* fusome, a germline-specific organelle, contains membrane skeletal proteins and functions in cyst formation. *Development*. 120:947–956.

Liu, J., M.A. Valencia-Sanchez, G.J. Hannon, and R. Parker. 2005. MicroRNA-dependent localization of targeted mRNAs to mammalian P-bodies. *Nat. Cell Biol.* 7:719–723.

Liu, J.L., and J.G. Gall. 2007. U bodies are cytoplasmic structures that contain uridine-rich small nuclear ribonucleoproteins and associate with P bodies. *Proc. Natl. Acad. Sci. USA*. 104:11655–11659.

Mahowald, A.P. 1971. Origin and continuity of polar granules. *In* Origin and Continuity of Cell Organelles. J. Reinert and H. Ursprung, editors. Springer-Verlag New York Inc., New York. 159–169.

Margolis, J., and A.C. Spradling. 1995. Identification and behavior of epithelial stem cells in the *Drosophila* ovary. *Development*. 121:3797–3807.

Megosh, H.B., D.N. Cox, C. Campbell, and H. Lin. 2006. The Role of PIWI and the miRNA machinery in *Drosophila* germline determination. *Curr. Biol.* 16:1884–1894.

Mohler, J., and S. Carroll. 1984. Report of new mutants. *Drosophila Information Service*. 60:236–241.

Morrison, S.J., and A.C. Spradling. 2008. Stem cells and niches: mechanisms that promote stem cell maintenance throughout life. *Cell*. 132:598–611.

Nakamura, A., R. Amikura, K. Hanyu, and S. Kobayashi. 2001. Me31B silences translation of oocyte-localizing RNAs through the formation of cytoplasmic RNP complex during *Drosophila* oogenesis. *Development*. 128:3233–3242.

Nicchitta, C.V., G. Migliaccio, and G. Blobel. 1991. Biochemical fractionation and assembly of the membrane components that mediate nascent chain targeting and translocation. *Cell*. 65:587–598.

Ponting, C.P. 1997. Tudor domains in proteins that interact with RNA. *Trends Biochem. Sci.* 22:51–52.

Reedy, M.C., and C. Beall. 1993. Ultrastructure of developing flight muscle in *Drosophila*. I. Assembly of myofibrils. *Dev. Biol.* 160:443–465.

Reedy, M.K., and M.C. Reedy. 1985. Rigor crossbridge structure in tilted single filament layers and flared-X formations from insect flight muscle. *J. Mol. Biol.* 185:145–176.

Rehwinkel, J., I. Behm-Ansmant, D. Gatfield, and E. Izaurralde. 2005. A crucial role for GW182 and the DCP1:DCP2 decapping complex in miRNA-mediated gene silencing. *RNA*. 11:1640–1647.

Rocak, S., and P. Linder. 2004. DEAD-box proteins: the driving forces behind RNA metabolism. *Nat. Rev. Mol. Cell Biol.* 5:232–241.

Rubin, G.M., and A.C. Spradling. 1982. Genetic transformation of *Drosophila* with transposable element vectors. *Science*. 218:348–353.

Ruohola, H., K.A. Bremer, D. Baker, J.R. Swedlow, L.Y. Jan, and Y.N. Jan. 1991. Role of neurogenic genes in establishment of follicle cell fate and oocyte polarity during oogenesis in *Drosophila*. *Cell*. 66:433–449.

Sambrook, J., E.F. Fritsch, and T. Maniatis. 1989. Transfer of proteins from SDS-polyacrylamide gels to solid supports: immunological detection of immobilized proteins (Western blotting). *In* Molecular Cloning: A Laboratory Manual. Second edition. Cold Spring Harbor Laboratory Press, Cold Spring Harbor, NY. 18.60–18.75.

Selenko, P., R. Sprangers, G. Stier, D. Buhler, U. Fischer, and M. Sattler. 2001. SMN tudor domain structure and its interaction with the Sm proteins. *Nat. Struct. Biol.* 8:27–31.

Sen, G.L., and H.M. Blau. 2005. Argonaute 2/RISC resides in sites of mammalian mRNA decay known as cytoplasmic bodies. *Nat. Cell Biol.* 7:633–636.

Sheth, U., and R. Parker. 2003. Decapping and decay of messenger RNA occur in cytoplasmic processing bodies. *Science*. 300:805–808.

Sprangers, R., M.R. Groves, I. Sinning, and M. Sattler. 2003. High-resolution X-ray and NMR structures of the SMN Tudor domain: conformational variation in the binding site for symmetrically dimethylated arginine residues. *J. Mol. Biol.* 327:507–520.

Wilhelm, J.E., M. Buszczak, and S. Sayles. 2005. Efficient protein trafficking requires *trailer hitch*, a component of a ribonucleoprotein complex localized to the ER in *Drosophila*. *Dev. Cell*. 9:675–685.

Wilsch-Bräuninger, M., H. Schwarz, and C. Nusslein-Volhard. 1997. A sponge-like structure involved in the association and transport of maternal products during *Drosophila* oogenesis. *J. Cell Biol.* 139:817–829.

Trentin, J.J. 1970. Influence of hematopoietic organ stroma (hematopoietic inductive microenvironments) on stem cell differentiation. *In* Regulation of Hematopoietic Stem Cells. A.S Gordon, editor. Appleton-Century-Crofts, New York. 161–185.

Xie, T., and A.C. Spradling. 1998. Decapentaplegic is essential for the maintenance and division of germline stem cells in the *Drosophila* ovary. *Cell*. 94:251–260.

Xie, T., and A.C. Spradling. 2000. A niche maintaining germ line stem cells in the *Drosophila* ovary. *Science*. 290:328–330.

Yang, Z., A. Jakymiw, M.R. Wood, T. Eystathioy, R.L. Rubin, M.J. Fritzler, and E.K. Chan. 2004. GW182 is critical for the stability of GW bodies expressed during the cell cycle and cell proliferation. *J. Cell Sci.* 117:5567–5578.

Young, M.W., and B.H. Judd. 1978. Nonessential sequences, genes, and the polytene chromosome bands of *Drosophila melanogaster*. *Genetics*. 88:723–742.

Zaccai, M., and H.D. Lipshitz. 1996. Differential distributions of two adducin-like protein isoforms in the *Drosophila* ovary and early embryo. *Zygote*. 4:159–166.